JNCI J Natl Cancer Inst (2020) 112(1): djz078

doi: 10.1093/jnci/djz078
First published online May 11, 2019
Article

ARTICLE

Uncovering the Role of RNA-Binding Protein hnRNP K in B-Cell Lymphomas

Miguel Gallardo,* Prerna Malaney,* Marisa J. L. Aitken, Xiaorui Zhang, Todd M. Link, Vrutant Shah, Sanzhar Alybayev, Meng-Han Wu, Laura R. Pageon, Huaxian Ma, Rodrigo Jacamo, Li Yu, Zijun Y. Xu-Monette, Haley Steinman, Hun Ju Lee, Dos Sarbassov, Inmaculada Rapado, Michelle C. Barton, Joaquin Martinez-Lopez, Carlos Bueso-Ramos, Ken H. Young, Sean M. Post

See the Notes section for the full list of authors' affiliations.
Correspondence to: Sean M. Post, PhD, The University of Texas, MD Anderson Cancer Center, 1515 Holcombe Blvd, MDA FC3.2002 (Unit 428), Houston, TX 77030 (e-mail: Spost@mdanderson.org).
*Authors contributed equally to this work.

Abstract

Background: Heterogeneous nuclear ribonucleoprotein K (hnRNP K) is an RNA-binding protein that is aberrantly expressed in cancers. We and others have previously shown that reduced hnRNP K expression downmodulates tumor-suppressive programs. However, overexpression of hnRNP K is the more commonly observed clinical phenomenon, yet its functional consequences and clinical significance remain unknown.
Methods: Clinical implications of hnRNP K overexpression were examined through immunohistochemistry on samples from patients with diffuse large B-cell lymphoma who did not harbor *MYC* alterations (n = 75). A novel transgenic mouse model that overexpresses hnRNP K specifically in B cells was generated to directly examine the role of hnRNP K overexpression in mice (three transgenic lines). Molecular consequences of hnRNP K overexpression were determined through proteomics, formaldehyde-RNA-immunoprecipitation sequencing, and biochemical assays. Therapeutic response to BET-bromodomain inhibition in the context of hnRNP K overexpression was evaluated in vitro and in vivo (n = 3 per group). All statistical tests were two-sided.
Results: hnRNP K is overexpressed in diffuse large B-cell lymphoma patients without *MYC* genomic alterations. This overexpression is associated with dismal overall survival and progression-free survival ($P < .001$). Overexpression of hnRNP K in transgenic mice resulted in the development of lymphomas and reduced survival ($P < .001$ for all transgenic lines; Line 171[n = 30]: hazard ratio [HR] = 64.23, 95% confidence interval [CI] = 26.1 to 158.0; Line 173 [n = 31]: HR = 25.27, 95% CI = 10.3 to 62.1; Line 177 [n = 25]: HR = 119.5, 95% CI = 42.7 to 334.2, compared with wild-type mice). Clinical samples, mouse models, global screening assays, and biochemical studies revealed that hnRNP K's oncogenic potential stems from its ability to posttranscriptionally and translationally regulate *MYC*. Consequently, *Hnrnpk* overexpression renders cells sensitive to BET-bromodomain-inhibition in both in vitro and transplantation models, which represents a strategy for mitigating hnRNP K-mediated c-Myc activation in patients.
Conclusion: Our findings indicate that hnRNP K is a bona fide oncogene when overexpressed and represents a novel mechanism for c-Myc activation in the absence of *MYC* lesions.

Heterogeneous nuclear ribonucleoprotein K (hnRNP K) is a single-stranded DNA (ssDNA) and RNA-binding protein that regulates a multitude of cellular processes via transcriptional, posttranscriptional, and translational mechanisms. Because of its pleotropic effects, increased as well as reduced expression have been implicated in disease processes (1–6). With specific

Received: March 26, 2018; **Revised:** March 22, 2019; **Accepted:** April 29, 2019

regard to increased expression, elevated hnRNP K levels have been observed in archived pathologic samples from patients with high-grade solid tumors (3,7–9). Additionally, hnRNP K has been implicated as a positive regulator of progrowth genes (ie, *SRC* and *EIF4E*) (10,11). These observations allude to an oncogenic function of hnRNP K. However, whether elevated hnRNP K levels can independently act as a driver of cancer remains unknown.

In the current manuscript, we assessed our working hypothesis that hnRNP K is a hitherto unknown oncogene with the capacity to drive neoplasms through diverse molecular programs including c-Myc. To investigate the oncogenic potential of hnRNP K, we focused on its role in a hematological malignancy where c-Myc is implicated: diffuse large B-cell lymphoma (DLBCL). Using DLBCL patient samples, we analyzed the impact that hnRNP K expression levels had on patient outcomes. To explore hnRNP K functions, we employed *Hnrnpk*-overexpressing transgenic mice and a host of molecular biology and biochemical assays to elucidate hnRNP K's role in lymphomagenesis.

Methods

Analysis of hnRNP K Expression Levels in DLBCL Patient Samples

Patient samples were obtained from the Histopathology Core at MD Anderson Cancer Center under institutional review board–approved protocols PA 11–0704 (CBR) and PA 11–0392 (KHY). Patient consent was obtained at the time of collection in accordance with the Declaration of Helsinki. Immunohistochemistry was performed as previously described (12), using antibodies against hnRNP K (3C2, Abcam). Two pathologists independently scored the hnRNP K expression.

Generation of Eμ-*Hnrnpk* Mice

The full-length *Hnrnpk* cDNA was cloned into the pBSV.E6BK vector (13), which was used to generate the Eμ-*Hnrnpk* transgenic mice. All mouse studies were conducted with approval from the Institutional Animal Care and Use Committee at MD Anderson under protocol 0000787-RN02.

Mass Spectrometry

Immunoprecipitation was performed using α-hnRNP K (Santa Cruz Biotechnology, D-6, Dallas, TX) or α-IgG (Abcam, ab18413, Cambridge, UK) using cytoplasmic and nuclear lysates from OCI-AML3 cells. Immunoprecipitated proteins were resolved by sodium dodecyl sulfate-polyacrylamide gel electrophoresis (SDS-PAGE), silver stained, and prepared for liquid chromatography-mass spectometry (LC-MS/MS) analysis. Proteins were identified by searching the fragment spectra against the Swiss-Prot protein database (EBI) using Mascot (Matrix Science, London, UK) or Sequest (Thermo Fisher Scientific, Waltham, MA).

Formaldehyde-RNA Immunoprecipitation (fRIP)

RNA samples for fRIP were prepared using a protocol described previously (14). The resulting RNA was then converted to cDNA and subjected to single-read sequencing on an Illumina HiSeq 2000 at a depth of 36 nucleotides per read at the MD Anderson Sequencing Core.

In Vitro BET-Bromodomain Inhibitor Assays

Splenocytes isolated from *Eμ-Hnrnpk* (n = 5) mice were treated with JQ1 (100, 300, or 1000 nM), ARV-825 (Arvinas Inc, New Haven, CT) (1, 3, or 10 nM), or vehicle (dimethyl sulfoxide [DMSO]) for 24 hours. Cell viability was measured at each harvest using trypan blue exclusion.

In Vivo BET-Bromodomain Inhibitor Assays

$Lin^{-}CD117^{+}$ cells from tumor-burdened *Eμ-Hnrnpk* mice (n = 3) were injected into matched pairs of irradiated female NSG mice (age 8–12 weeks). Engrafted mice were treated with vehicle (DMSO in 10% HP-β-CD) or JQ1 (50 mg/kg delivered in DMSO and 10% HP-β-CD). After three weeks of treatment, mice were killed. Evaluation of lymphocytes by flow cytometry and complete blood count (CBC) was performed pre- and posttreatment.

Statistical Analysis

Statistical analyses were performed using Student *t* tests or Mann-Whitney tests. Survival analysis and comparison of curves was performed using the Kaplan-Meier estimator and log-rank test, respectively. Hazard ratios were obtained via the Mantel-Haenszel method. *P* values less than 0.05 were considered statistically significant. All statistical tests were two-sided.

Detailed descriptions are provided in Supplementary Materials (available online).

Results

hnRNP K Levels in Patients With DLBCL

To examine whether alterations in hnRNP K expression affect patients with lymphoid malignancies, we screened samples from patients with de novo DLBCL without *MYC* genomic alterations. *HNRNPK* RNA levels were elevated in $CD19^{+}$ B cells from patients with lymphoma (n = 15) compared with healthy donors (n = 9, $P = .04$) (Figure 1, A). hnRNP K protein expression was also found to be elevated in lymph node and bone marrow biopsies from patients with DLBCL in 7 of 10 samples compared with controls (activated lymph nodes from healthy donors undergoing tonsillectomy) (Figure 1, B). Furthermore, stratifying DLBCL patient samples (n = 75) by high (n = 46) or low (n = 29) hnRNP K expression showed that patients with high hnRNP K expression had a statistically significant decrease in overall survival (OS) and progression-free survival (PFS) (median OS and PFS at <25 months [high hnRNP K] vs median not reached at >200 months [low hnRNP K], $P < .001$ and $P < .001$, respectively) (Figure 1, C and D; Supplementary Figure 1, A, available online). Increased hnRNP K expression was also associated with poor outcomes both in germinal B-cell (GBC) and activated B-cell (ABC) subtypes of DLBCL and a lack of complete remission (Table 1; Supplementary Figure 1, B and C, and Supplementary Table 1, available online). hnRNP K expression was not elevated in *MYC* rearranged cases compared with cases with normal fluorescence in situ hybridization or polysomy cases ($P = .43$). Together, these results indicate that hnRNP K is overexpressed in a large subset of patients with DLBCL that do not harbor *MYC*

ARTICLE

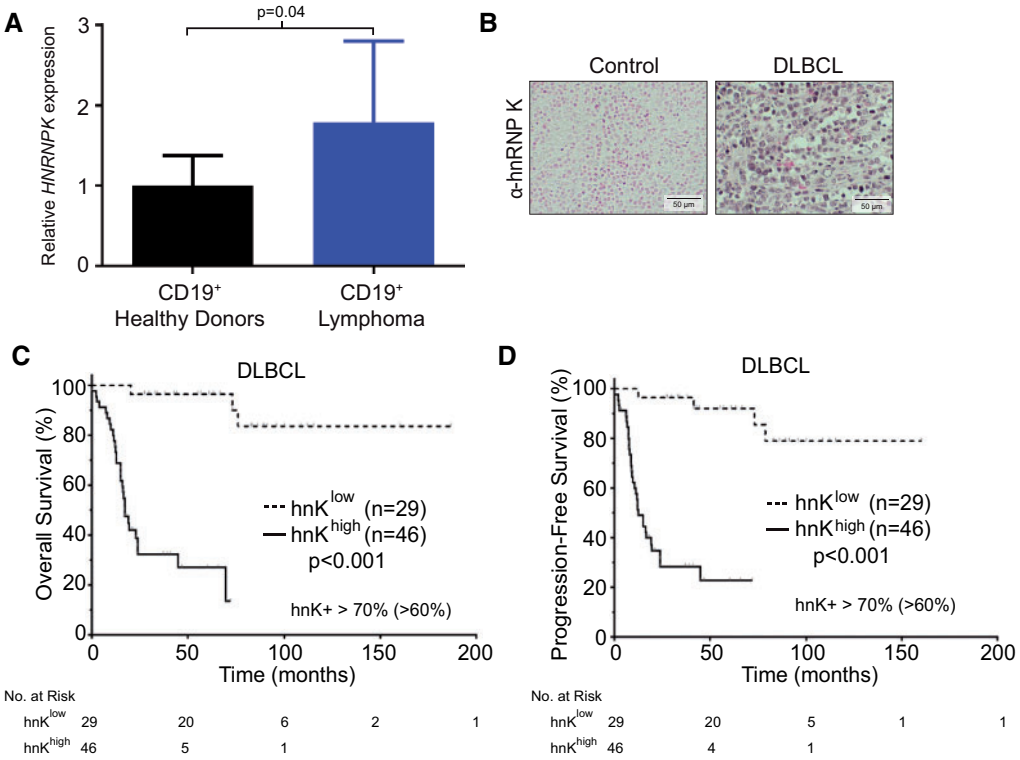

Figure 1. hnRNP K expression levels in DLBCL patient samples. **A)** Quantitative RT-PCR analysis of *HNRNPK* levels in CD19$^+$ B cells isolated from patients with lymphoma (n = 15) and healthy donors (n = 9). Data are represented as the mean ± SD as determined from triplicate samples after normalization to *GAPDH* expression. *P* values were calculated using a two-sided Student *t* test. **B)** Immunohistochemical analyses of hnRNP K levels in activated lymph nodes of healthy donors (tonsils) and in lymph nodes of patients with DLBCL. The scale bar represents 50 μm. **C)** Kaplan-Meier curve representing overall survival of patients with DLBCL based on high hnRNP K expression (n = 46) compared with patients with weak or low expression (n = 29). Statistical significance was determined by a two-sided log-rank test. **D)** Kaplan-Meier curve representing progression-free survival of patients with DLBCL based on high hnRNP K expression (n = 46) compared with patients with weak and/or low expression (n = 29). Statistical significance was determined by a two-sided log-rank test. DLBCL = diffuse large B-cell lymphoma; hnK = heterogeneous nuclear ribonucleoprotein K (hnRNP K); RT-PCR = reverse transcription polymerase chain reaction.

genomic alterations, and this overexpression is associated with poor clinical outcomes, suggesting that hnRNP K overexpression may underlie B-cell lymphomagenesis.

Generation and Phenotypic Analysis of Eμ-*Hnrnpk* Transgenic Mice

To directly examine the impact of hnRNP K overexpression in vivo, we generated three lines of transgenic mice that overexpress hnRNP K specifically in the B-cell compartment (Eμ-*Hnrnpk*, Lines 171, 173, and 177) (Figure 2, A–D; Supplementary Figure 2, A–C, available online).

Phenotypically, Eμ-*Hnrnpk* mice exhibited a statistically significant reduction in survival across all transgenic lines compared with wild-type mice ($P < .001$ for all lines; Line 171 [n = 30]: hazard ratio [HR] = 64.23, 95% confidence interval [CI] = 26.1 to 158.0; Line 173 [n = 31]: HR = 25.27, 95% CI = 10.3 to 62.1; Line 177 [n = 25]: HR = 119.5, 95% CI = 42.7 to 334.2, compared with wild-type mice [n = 64]) (Figure 3A).Gross analyses of moribund mice revealed that Eμ-*Hnrnpk* mice had a 12-fold increase in splenic weight ($P = .006$) and a 3.5-fold increase in hepatic weight ($P = .01$) (Figure 3, B–E). To more precisely characterize these malignancies, we performed flow cytometric, morphologic, and immunohistochemical analyses. Eμ-*Hnrnpk* mice primarily displayed one of two distinct immunophenotypes as assessed by flow cytometry. Six of 10 mice expressed the surface markers B220^{hi} CD43$^+$ CD24$^+$, which is suggestive of a pre-B-cell. The remaining four mice displayed a B220^{lo} CD43$^+$ CD24$^+$ immunophenotype, indicating a more immature B cell (Supplementary Figure 3A, available online). These results are reminiscent of Eμ-*Myc* mice, which often exhibit heterogeneous immunophenotypes (15–18). Morphologically, we observed loss of splenic architecture in diseased Eμ-*Hnrnpk* spleens compared with wild-type mice (Figure 3F, hematoxylin and eosin staining) and expansion of B-cell lineage markers (Figure 3F, PAX5 staining). Additionally, we observed invasion of B cells throughout the liver (Figure 3G, B220 staining), with only marginal T-cell infiltration (Figure 3G, CD3 staining). In addition to their invasive nature, Eμ-*Hnrnpk*-dependent lymphomas were highly proliferative as determined by elevated Ki67 levels (Figure 3F). Taken together, these data indicate that hnRNP K overexpression directly contributes to lymphomagenesis and that hnRNP K is a bona fide oncogene when overexpressed.

Even though lymphomas typically reside within hematopoietic tissues, they can extravasate into the peripheral blood. CBC analyses and Wright staining of peripheral blood from Eμ-*Hnrnpk* mice showed a statistically significant increase in large unstained cells (LUC) when compared with wild-type mice (mean [SD] =12.2 [2.1]%, (n = 23) vs mean [SD] = 1.3 [0.2]% (n = 10), respectively, $P = .002$) (Figure 3, H). To identify components that contribute to cell migration and proliferation, we examined cytokine levels in the serum of mice. Compared with wild-type mice (n = 4), Eμ-*Hnrnpk* mice (n = 6) had a statistically significant increase in the lymphocytic proliferative cytokine

Table 1. Clinicopathologic characteristics of patients with diffuse large B-cell lymphoma (DLBCL) with low or high levels of hnRNP K expression

Characteristic	DLBCL			GCB-DLBCL			ABC-DLBCL		
	hnRNP K^{high} No. (%)	hnRNP K^{low} No. (%)	P*	hnRNP K^{high} No. (%)	hnRNP K^{low} No. (%)	P*	hnRNP K^{high} No. (%)	hnRNP K^{low} No. (%)	P*
Age, y									
<60	15 (32.6)	12 (41.4)	.47	7 (36.8)	9 (56.3)	.32	8 (29.6)	3 (23.1)	1.0
≥60	31 (67.4)	17 (58.6)		12 (63.2)	7 (43.8)		19 (70.4)	10 (76.9)	
Sex									
Male	25 (54.3)	19 (65.5)	.47	11 (57.9)	10 (62.5)	1.0	14 (51.9)	9 (69.2)	.33
Female	21 (45.7)	10 (34.5)		8 (42.1)	6 (37.5)		13 (48.1)	4 (30.8)	
Stage									
I–II	16 (37.2)	16 (55.2)	.15	12 (66.7)	9 (56.3)	.73	4 (16.0)	7 (53.8)	.02
III–IV	27 (62.7)	13 (44.8)		6 (33.3)	7 (43.8)		21 (84.0)	6 (46.2)	
B symptoms									
No	25 (61.0)	20 (74.1)	.31	13 (76.5)	11 (73.3)	1.0	12 (50.0)	9 (75.0)	.28
Yes	16 (39.0)	7 (25.9)		4 (23.5)	4 (26.7)		12 (50.0)	3 (25.0)	
Serum LDH levels									
Normal	17 (47.2)	13 (52.0)	.80	8 (57.1)	9 (64.3)	1.0	9 (40.9)	4 (36.4)	1.0
Elevated	19 (52.8)	12 (48.0)		6 (42.9)	5 (35.7)		13 (59.1)	7 (63.6)	
No. of extranodal sites									
0 or 1	34 (73.9)	26 (89.7)	.14	14 (73.7)	14 (87.5)	.42	20 (74.1)	12 (92.3)	.24
≥2	12 (26.1)	3 (10.3)		5 (26.3)	2 (12.5)		7 (25.9)	1 (7.7)	
ECOG performance status									
0 or 1	24 (66.7)	22 (88.0)	.07	9 (64.3)	13 (92.9)	.17	15 (68.2)	9 (81.8)	.68
≥2	12 (33.3)	3 (12.0)		5 (35.7)	1 (7.1)		7 (31.8)	2 (18.2)	
Largest tumor size, cm									
<5	18 (52.9)	10 (58.8)	.77	9 (60.0)	6 (60.0)	1.0	9 (47.4)	4 (57.1)	1.0
≥5	16 (47.1)	7 (41.2)		6 (40.0)	4 (40.0)		10 (52.6)	3 (42.9)	
IPI risk group									
0–2	21 (50.0)	22 (78.6)	.02	11 (64.7)	12 (80.0)	.44	10 (40.0)	10 (76.9)	.04
3–5	21 (50.0)	6 (21.4)		6 (35.3)	3 (20.0)		15 (60.0)	3 (23.1)	
Therapy response									
Complete response	23 (50.0)	26 (96.3)	<.001	12 (63.2)	16 (100.0)	.009	11 (40.7)	12 (92.3)	.002
Noncomplete response	23 (50.0)	1 (3.7)		7 (36.8)	0 (0.0)		16 (59.3)	1 (7.7)	

*Characteristics are compared by Fisher exact test. P values are two-sided. ABC = activated B-cell–like; ECOG = Eastern Cooperative Oncology Group; GCB = germinal center B-cell–like; hnRNP K = heterogeneous nuclear ribonucleoprotein K; LDH = lactate dehydrogenase; IPI = International Prognostic Index.

ARTICLE

interleukin-9 (IL-9), consistent with observations in DLBCL patients (19) ($P < .001$) (Figure 3I). Together, these findings indicate that hnRNP K overexpression promotes the development of B-cell lymphomas that have the potential to extravasate into the peripheral blood.

Assessing Transplantability of Cells From Eμ-*Hnrnpk* Mice

To better understand the malignant nature of Eμ-*Hnrnpk* cells, we performed transplantation experiments (Figure 4, A). Mice transplanted with Eμ-*Hnrnpk* cells had a statistically significant decrease in survival compared with recipients of wild-type cells (HR = 13.19, 95% CI = 2.5 to 69.1 for Eμ-*Hnrnpk* cell recipients, wild-type cell recipients survived until the end of the study [day 100], $P = .002$) (Figure 4B). CBC analyses showed a statistically significant increase in the number of LUCs in mice transplanted with Eμ-*Hnrnpk* cells ($P = .046$) (Figure 4C), recapitulating the phenotypes observed in Eμ-*Hnrnpk* transgenic mice. Taken together, these experiments support the cell-autonomous nature of Eμ-*Hnrnpk* cells for driving malignant phenotypes.

Global Analyses to Delineate hnRNP K Function

Our clinical and in vivo observations provide firm evidence that hnRNP K acts as an oncogene when overexpressed. Given its lack of enzymatic activity, we postulated that hnRNP K functions as an oncogene via its DNA-binding (transcriptional), RNA-binding (posttranscriptional) functions or through protein-protein interactions that alter signaling cascades (2,20,21). Consequently, we performed mass spectrometry to identify proteins associated with hnRNP K. hnRNP K predominantly bound to RNA-processing and ribosomal proteins, insinuating that hnRNP K may regulate genes primarily at a posttranscriptional level (Supplementary Figure 4, A–C, available online). We next performed formaldehyde RNA-immunoprecipitation experiments (fRIP) to identify transcripts bound to hnRNP K. fRIP-Seq experiments revealed that hnRNP K was associated with a number of transcripts implicated in cancer progression (22) (Supplementary Figure 4D, available online). When cross-referenced with known tumor suppressive and oncogenic transcripts implicated in lymphomagenesis (23), the *MYC* transcript emerged as an important immunoprecipitant of hnRNP K (Figure 5A). Importantly, our fRIP data revealed an association between hnRNP K and the *MYC*

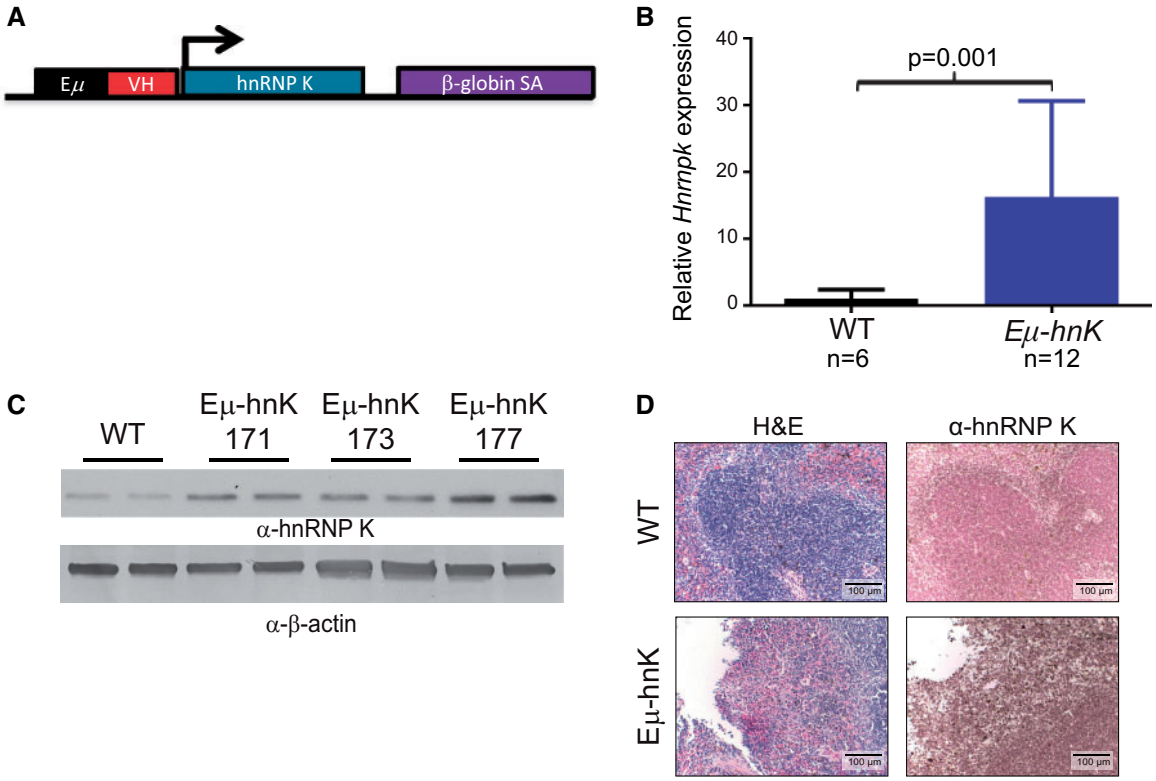

Figure 2. Generation of *Eμ-Hnrnpk* mice. **A)** Schema of the *Eμ-Hnrnpk* transgenic cassette. The *Hnrnpk* cDNA was placed downstream of the Eμ immunoglobulin heavy-chain enhancer. **B)** Quantitative RT-PCR analysis of *Hnrnpk* levels in the spleens of *Eμ-Hnrnpk* (n = 12) and wild-type (n = 6) mice. Data are represented as the mean ± SD after normalization to *RPLP0* expression levels. *P* values were calculated using a two-sided Mann-Whitney test. **C)** Immuno blot analyses of hnRNP K levels in splenic samples isolated from wild-type and *Eμ-Hnrnpk* mice (transgenic lines 171, 173, and 177). *β*-actin expression serves as a loading control. Each lane represents lysate from an individual animal. **D)** Hematoxylin and eosin (H&E) staining and immunohistochemical analyses of hnRNP K levels in splenic samples isolated from wild-type and *Eμ-Hnrnpk* mice. The scale bar represents 100 μm. hnK = heterogeneous nuclear ribonucleoprotein K (hnRNP K); RT-PCR = reverse transcription polymerase chain reaction; VH = heavy chain variable region; WT = wild-type.

internal ribosome entry site (IRES) and exon 2 of the *MYC* coding sequence (Supplementary Figure 4E, available online). Using a Burkitt lymphoma cell line (Ramos) and murine splenic lysates, we confirmed these hnRNP K/*MYC* interactions via native RNA-immunoprecipitation assays (RIP) ($P < .001$ and $P = .03$, respectively) (Figure 5, B and C; Supplementary Figure 4F, available online).

Because RIP cannot exclude the possibility of a multiprotein complex containing other RNA-binding proteins, we sought to determine whether the hnRNP K/*MYC* interaction was direct. Using a computer-based algorithm, we scanned the *MYC* transcript for putative hnRNP K-binding sites and identified potential novel hnRNP K-binding motifs in the *MYC* IRES and the second exon of the *MYC* transcript, consistent with our fRIP analyses. To test for direct binding between hnRNP K and RNA, we performed fluorescence anisotropy assays using recombinant hnRNP K protein (Supplementary Figure 4, G and H, available online). Here, we observed a specific and stringent interaction between hnRNP K and the *MYC* IRES and the *MYC* exon 2 sequence (Figure 5, D and E; Supplementary Figure 4I, available online), which was lost when the hnRNP K consensus sites were mutated.

Elucidating hnRNP K's Impact on c-Myc Expression

Increased c-Myc expression, a critical hallmark in the pathogenesis of lymphomas, is often attributed to *MYC* translocations or amplification. However, *MYC* rearrangements in de novo DLBCL occur at frequencies well below the incidence of c-Myc overexpression (24–26), indicating that alternate mechanisms that increase c-Myc expression must exist. Given our observations that hnRNP K directly interacts with the *MYC* transcript, we hypothesized that hnRNP K overexpression represents a novel mechanism to increase c-Myc levels in the absence of *MYC* genomic lesions. To examine this, we evaluated c-Myc expression levels in our models and observed increased c-Myc expression in mice (Figure 6A; Supplementary Figure 5A, available online) and DLBCL patient samples that did not carry *MYC* alterations ($P = .01$) (Figure 6, B and C). Conversely, hnRNP K knockdown resulted in a decrease in c-Myc expression in Ramos cells and 293T cells (Figure 6, D and E), indicating that hnRNP K may regulate c-Myc levels.

Next, we sought to determine the mechanisms underlying hnRNP K-mediated c-Myc regulation. We investigated the effect of hnRNP K on *MYC* at transcriptional, posttranscriptional, and translational levels. In DLBCL patient samples, as well as samples from healthy and diseased *Eμ-Hnrnpk* mice, *MYC* RNA levels remained unchanged compared with corresponding controls ($P = .90$, $P = .84$, and $P = .20$, respectively) (Supplementary Figure 5,B–D, available online). Therefore, the increase in c-Myc protein expression was not reflective of a concomitant increase in *MYC* RNA. To further examine any potential role in transcription, we used luciferase-based transcriptional assays and observed that hnRNP K had only a modest effect on the *MYC* promoter (Supplementary Figure 5, E and F, available online),

ARTICLE

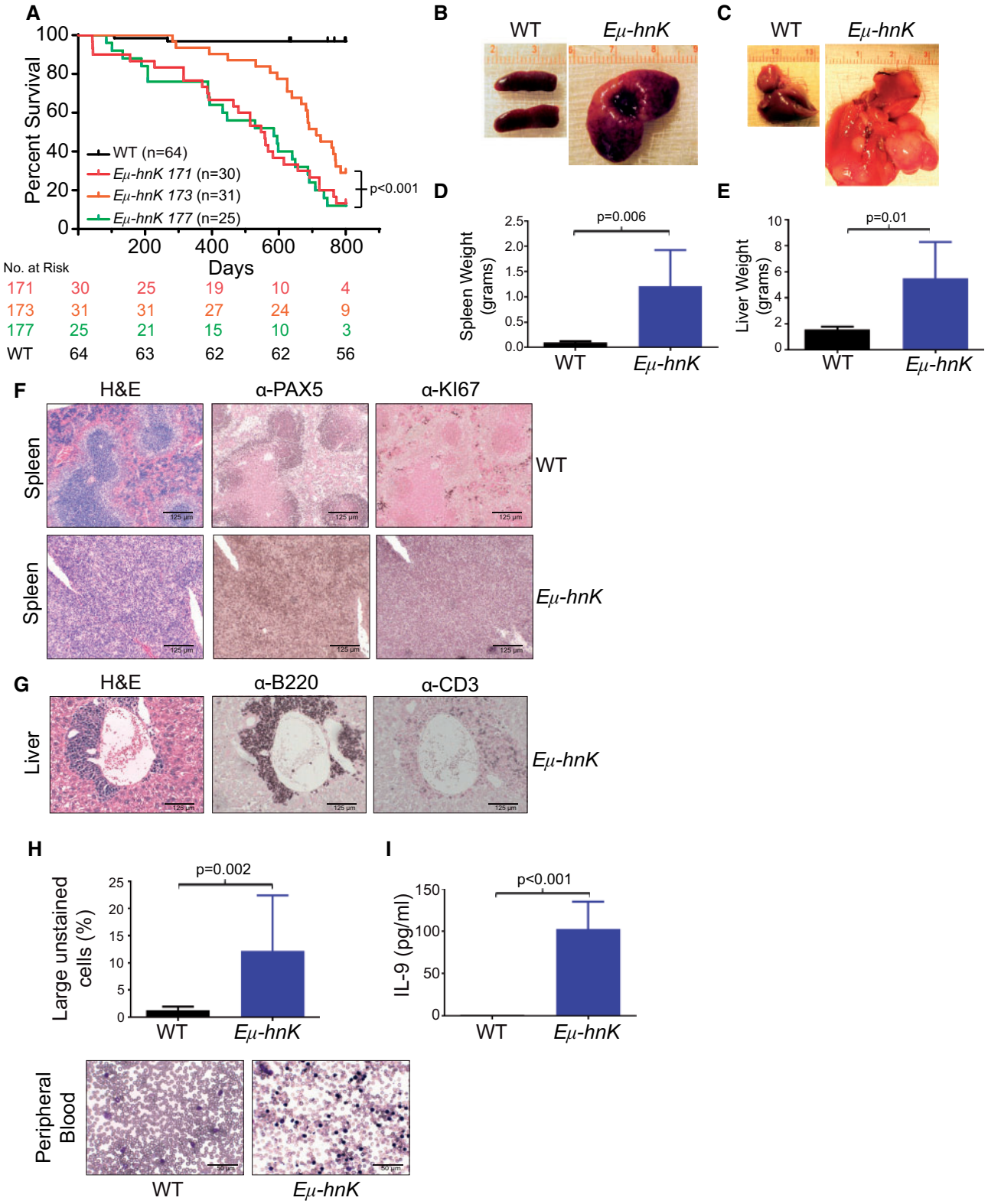

Figure 3. Phenotypic characterization of Eμ-*Hnrnpk* transgenic mice. **A)** Kaplan-Meier curves indicating survival of Eμ-*Hnrnpk* lines 171 (n = 30), 173 (n = 31), 177 (n = 25), and wild-type (n = 64) mice. Statistical significance was determined by a two-sided log-rank test. Representative photos of spleens **(B)** and livers **(C)** from Eμ-*Hnrnpk* and wild-type mice. **D)** Bar graphs depicting spleen **(D)** and liver **(E)** weights from Eμ-*Hnrnpk* and wild-type mice. Data are represented as the mean ± SD. *P* values were calculated using a two-sided Student *t* test. **F)** H&E and immunohistochemical staining of splenic sections from wild-type and disease-burdened Eμ-*Hnrnpk* mice with PAX5 (B-cell marker) and Ki67 (proliferation marker). The scale bar represents 125 μm. **G)** H&E and immunohistochemical staining of livers with B-cell infiltrates from Eμ-*Hnrnpk* mice diagnosed with lymphoma ($B220^+/CD3^-$). The scale bar represents 125 μm. **H)** Bar graph representing large unstained cells (LUC) from peripheral blood of Eμ-*Hnrnpk* (n = 23) and wild-type (n = 10) mice. Data are represented as the mean ± SD. *P* values were calculated using a two-sided Student *t* test. Wright-Giemsa staining of representative peripheral blood from Eμ-*Hnrnpk* and wild-type mice. The scale bar represents 50 μm. **I)** Bar graph representing cytokine concentrations of interleukin-9 (IL-9) in the peripheral blood of wild-type (n = 4) and Eμ-*Hnrnpk* mice (n = 6) diagnosed with lymphoma. Data are represented as the mean ± SD. *P* values were calculated using a two-sided Student *t* test. H&E = hematoxylin and eosin; hnK = heterogeneous nuclear ribonucleoprotein K (hnRNP K); WT = wild-type.

ARTICLE

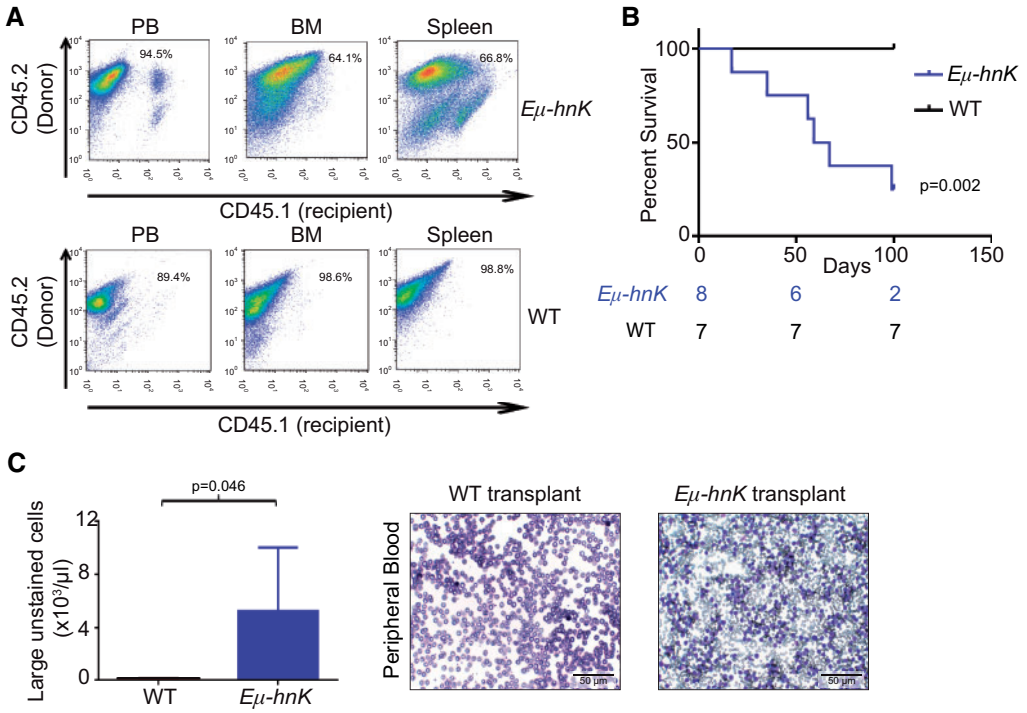

Figure 4. Transplantation of Eμ-*Hnrnpk* cells in mice. **A)** Flow cytometry analysis of CD45.1$^+$ (recipient) and CD45.2$^+$ (donor) hematopoietic cells in the peripheral blood (**left panels**), bone marrow (**center panels**), and spleen (**right panels**) of recipient mice following transplantation of cells from Eμ-*Hnrnpk* (**top panels**) and wild-type (**bottom panels**) mice. **B)** Kaplan-Meier curves indicating survival of NSG mice transplanted with either Eμ-*Hnrnpk* (n = 8) or wild-type (n = 7) cells. Statistical significance was determined by a two-sided log-rank test. **C)** Bar graph representing the population of large unstained cells (LUC) from complete blood count analyses of NSG mice transplanted with cells from Eμ-*Hnrnpk* (n = 4) and wild-type (n = 4) mice. Data are represented as the mean ± SD. *P* values were calculated using a two-sided Student *t* test. Wright-Giemsa staining of representative peripheral blood from NSG mice transplanted with cells from Eμ-*Hnrnpk* or wild-type mice. The scale bar represents 50 μm. BM = bone marrow; NSG = NOD scid gamma; PB = peripheral blood; WT = wild-type.

suggesting that in this context, hnRNP K primarily exerts its influence on c-Myc expression posttranscriptionally.

RNA-immunoprecipitation and fluorescence anisotropy assays, described above, show that hnRNP K bound the *MYC* transcript within its IRES and coding sequence. To determine the functional consequence of the hnRNP K MYC interaction, we performed RNA stability assays. hnRNP K overexpression in 293T cells increased stability of the *MYC* transcript ($t_{1/2}$: 76 minutes [hnRNP K] vs $t_{1/2}$: 46 minutes [control]) (Figure 6F; Supplementary Figure 5G, available online). Further, the presence of hnRNP K binding sites in the IRES of the *MYC* transcript alludes to a role for hnRNP K in regulating *MYC* ribosomal loading (27). To assess the effect of hnRNP K in regulating the translation of *MYC* mRNA, we performed polysome assays in 293T cells and observed a global change in the translational profile of cells transfected with si*HNRNPK*. Specifically, there was a dramatic increase in the monosomes accompanied by a minimal decrease in the polysome fractions (Figure 6G), consistent with previously published data (27). Although hnRNP K knockdown caused a global increase in the monosome fraction, there was a statistically significant decrease in the amount of *MYC* mRNA bound to monosomes, (Figure 6H), suggesting that there may be defective loading of the *MYC* mRNA onto the ribosomes when hnRNP K levels are reduced. We next used a luciferase-based reporter system to assess the effects of hnRNP K on the *MYC* IRES in vitro. Luciferase-reporters containing the entire *MYC* IRES or a short stretch of the *MYC* IRES (used in our fluorescence anisotropy assays) showed greater luciferase activity compared with the empty vector controls and the reporter containing the *MYC* IRES with mutated hnRNP K sites (Supplementary Figure 5H, available online). These results indicate that hnRNP K interacts with, stabilizes, and influences the ribosomal loading of the *MYC* transcript. Together, these effects contribute to elevated c-Myc expression. Our studies, therefore, reveal a novel mechanism for driving c-Myc expression when the *MYC* locus is neither amplified nor translocated.

Assessing the Efficacy of Bromodomain Inhibition in hnRNP K-Dependent B-Cell Lymphomas

Given that hnRNP K overexpression directly contributes to the expression of c-Myc in vivo, we next sought to investigate whether these effects could be therapeutically mitigated. Although no drug currently exists for directly targeting hnRNP K's interactions with *MYC*, BET-bromodomain inhibitors such as JQ1 (28) and BRD4-PROTACs such as ARV-825(29), both of which inhibit *MYC* transcription and consequently reduce the amount of transcript available to be translated (30), have been shown to be effective in tumors with elevated c-Myc. Thus, in the context of hnRNP K overexpression, reducing the pool of *MYC* transcripts may be an effective way to mitigate hnRNP K's oncogenic functions. To assess this, we treated splenocytes from Eμ-*Hnrnpk* mice (n = 5) with increasing doses of JQ1 or ARV-825 and observed a statistically significant decrease in viability at 24 (Figure 7A), 48, and 72 hours (Figure 7B) compared with vehicle (DMSO).

To examine the efficacy of bromodomain inhibitors in vivo, we treated CD45.1$^+$ NSG mice transplanted with CD45.2$^+$ Eμ-*Hnrnpk* cells with JQ1 for 21 days and observed a statistically

ARTICLE

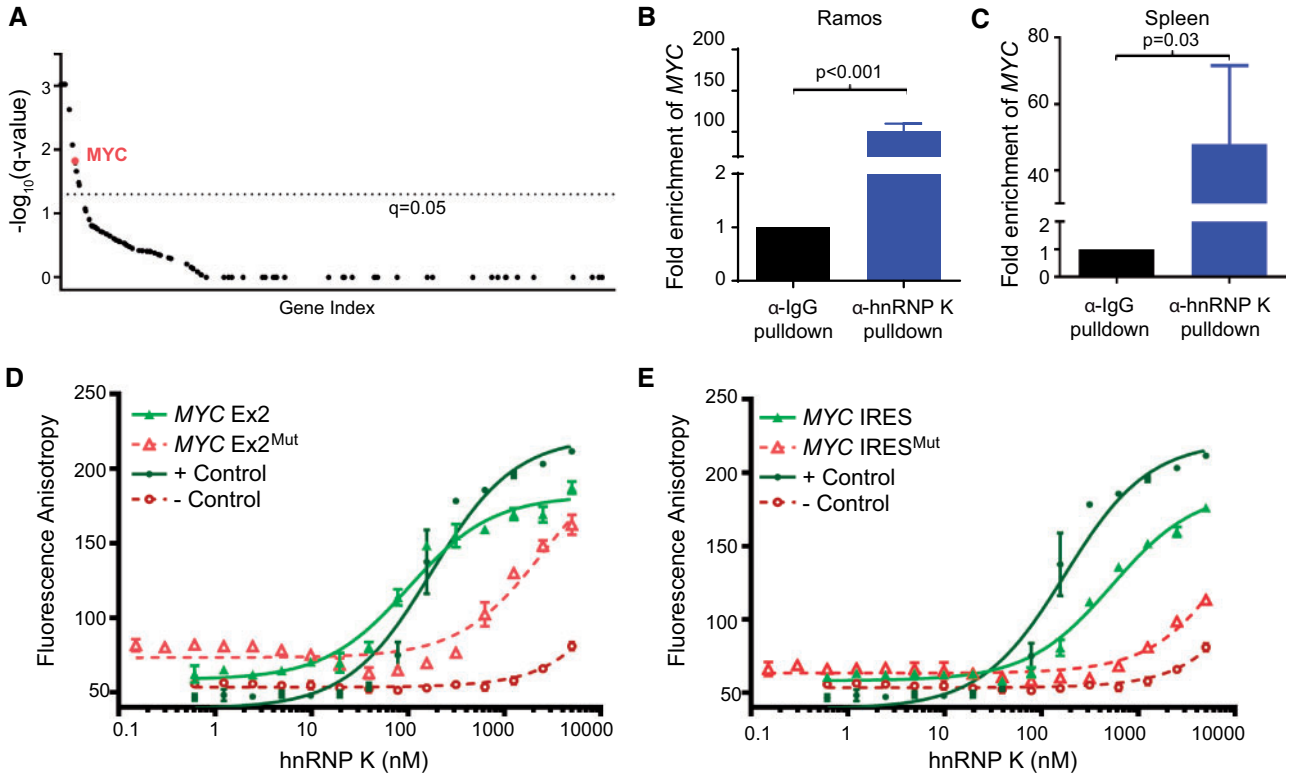

Figure 5. Global analyses of the RNA-binding functions of hnRNP K. **A)** Graph depicting hnRNP K-associated transcripts, as determined by fRIP analysis, subsetted by causal implication in lymphoma. Transcripts associated with lymphoma were identified using published papers (22, 23). The fRIP-Seq experiments were performed in triplicate in OCI-AML3 cells and a cutoff representing a q-value of 0.05 is indicated as a dotted line. **B and C)** Bar graphs representing relative fold enrichment of the interaction between the *MYC* transcript and α-hnRNP K and α-IgG immunoprecipitates in RNA-immunoprecipitation (RIP) assays in Ramos cells (**left panels**) and murine spleens (n = 3) (**right panels**). Data are represented as the mean ± SD as determined from triplicate samples after normalization to 10% input. *P* values were calculated using a two-sided Student *t* test. **D and E)** Fluorescence anisotropy binding curves for purified full-length hnRNP K with FAM-labeled *MYC* Exon2 and *MYC* IRES wild-type and mutant oligos. Curves for the positive and negative controls are also included. Binding assays were performed in triplicate. IgG = immunoglobulin G; IRES = internal ribosome entry site; fRIP = formaldehyde-fixed RNA-immunoprecipitation; hnRNP K = heterogeneous nuclear ribonucleoprotein K; RIP = RNA-immunoprecipitation.

ARTICLE

significant reduction in the number of $CD45.2^+$ donor cells in the transplanted NSG mice ($P = .045$, n = 3) (Figure 7, C and D) and reduced tumor burden in the spleen compared to the vehicle control ($P = .03$, n = 3) (Figure 7E). Mechanistically, we observed that JQ1 reduced c-Myc protein levels in OCI-AML3 and Ramos cell lines as previously published (31) (Figure 7, F and G). Intriguingly, JQ1 treatment also resulted in a moderate reduction in hnRNP K protein levels (Figure 7, F and G). Using RNA-immunoprecipitation assays, we observed a reduced interaction between hnRNP K and the *MYC* transcript following JQ1 treatment (Figure 7, H and I). However, this is likely due to reduced *MYC* transcript levels on JQ1 treatment, which limits the pool of *MYC* transcript available to hnRNP K (Supplementary Figure 6,A and B, available online). JQ1 did not to appear to affect the efficiency of the interaction of hnRNP K to *MYC* (Supplementary Figure 6, C and D, available online), suggesting JQ1 does not inhibit the hnRNP K/MYC interaction. Even though we are currently unable to directly target hnRNP K or c-Myc in vivo, JQ1 indirectly targets these oncogenic molecules, and these results demonstrate the efficacy of BET-bromodomain inhibitors in hnRNP K and c-Myc-overexpression-dependent B-cell malignancies.

Discussion

In this study, we evaluate the role of hnRNP K overexpression in lymphomagenesis. Herein, we observed that DLBCL patients with high hnRNP K expression suffered poor clinical outcomes compared with patients with lower hnRNP K levels. Mouse models that specifically overexpress hnRNP K in the B-cell compartment exhibited a highly penetrant lymphoma phenotype and had reduced survival compared with wild-type mice. Molecularly, we observed that high hnRNP K expression resulted in increased c-Myc levels in mouse models and DLBCL patient samples. Mechanistically, we observed that hnRNP K exerts oncogenic functions through posttranscriptional and translational regulation of the *MYC* transcript. These results suggest that overexpression of hnRNP K may force c-Myc expression and contribute to the pathogenesis of DLBCL in the absence of *MYC* genomic aberrations. Taken together, our results indicate that hnRNP K behaves as an oncogene when overexpressed.

In contrast to our current observations, we and others have previously demonstrated that haploinsufficiency or reduced hnRNP K expression also contributes to tumor development by dampening the response of the p53 pathway (4,6,32,33). Reconciling hnRNP K's tumor-suppressive and oncogenic roles is perplexing, but extant literature offers insights into the rationale behind hnRNP K's dual functionality. First, hnRNP K is a highly pleiotropic RNA and ssDNA-binding protein that influences transcription, translation, and splicing. Thus, perturbations in its expression may lead to the inappropriate expression of target proteins resulting in growth or differentiation advantages. This pleiotropy offers a plausible rationale for the

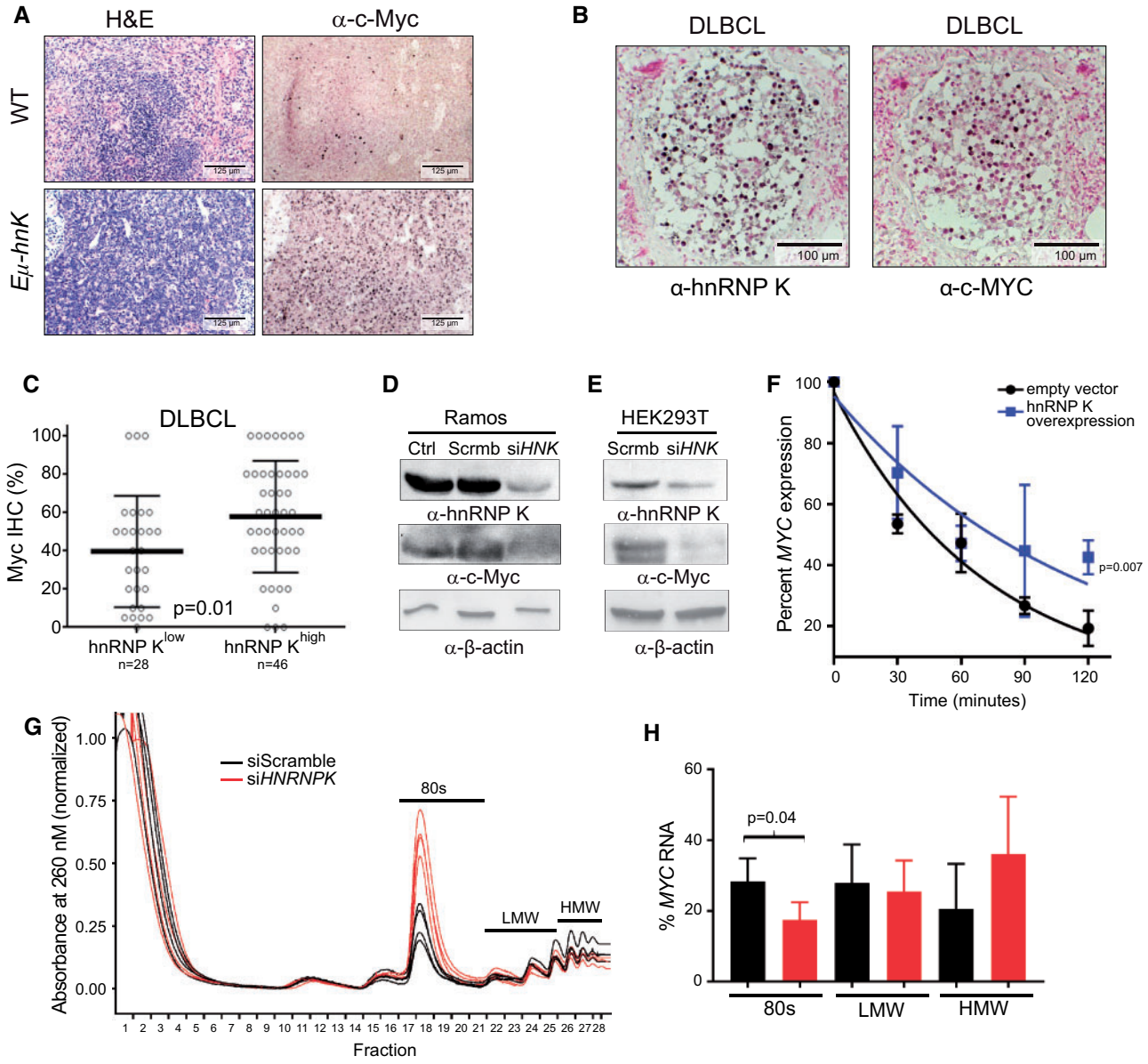

Figure 6. Assessing hnRNP K's impact on c-Myc expression. **A)** H&E and immunohistochemical analyses of c-Myc levels in spleen samples isolated from wild-type and Eμ-*Hnrnpk* mice. The scale bar represents 125 μm. **B)** Immunohistochemical analyses of hnRNP K and c-Myc levels in lymph nodes and bone marrow of DLBCL patients. The scale bar represents 100 μm. **C)** Bar graph representing c-Myc protein as function of high (n = 46) or low (n = 28) hnRNP K in patients with DLBCL without concomitant *MYC* alterations. Error bars represent SD from the mean. *P* values were calculated using a two-sided Student *t* test. **D and E)** Immuno blot analyses of hnRNP K and c-Myc expression following siRNA-mediated knockdown of hnRNP K (siHNK) or scrambled si-RNAs (Scrmb) in Ramos and HEK293T cells. *β*-actin expression serves as a loading control. **F)** Graph representing *MYC* transcript levels in 293T cells transfected with control and Flag-hnRNP K plasmids on actinomycin treatment. *RPLP0* serves as an internal control. All time points were performed in triplicate. *P* values were calculated using a two-sided Student *t* test. **G)** Polysome assay trace for 293T cells transfected with siScramble or siHNRNP K on a 0%–50% sucrose gradient. **H)** Graph representing percent *MYC* mRNA levels in various ribosomal components as determined by qRT-PCR. Data are represented as the mean ± SD. *P* values were calculated using a two-sided Student *t* test. DLBCL = diffuse large B-cell lymphoma; H&E = hematoxylin and eosin; HMW = high molecular weight; hnRNP K = heterogeneous nuclear ribonucleoprotein K; IHC = immunohistochemistry; LMW = low molecular weight; qRT-PCR = quantitative reverse transcription polymerase chain reaction; WT = wild-type.

observation that loss (34–38) and gains (39–41) in expression negatively affect clinical outcomes and disease. Second, it is entirely plausible that an insufficiency of hnRNP K allows for paths to tumorigenesis distinct from that of overexpression, as *HNRNPK* loss results in diminished activation of tumor suppressors (4,6,32), whereas overexpression of hnRNP K has been linked to activation of proliferative programs (10,42). These observations suggest that hnRNP K may have its hand both on the throttle and the brake of cellular programs that influence tumor formation and that any changes in its expression may result in neoplastic formation.

Although these dual oncogenic and tumor-suppressive functions are biologically interesting, dose-dependent events also create a perplexing therapeutic challenge. A prudent treatment strategy for tumors harboring alterations in proteins with dual tumor suppressor/oncogenic functions must be context-specific. In the context of hnRNP K overexpression, directly targeting hnRNP K or ablating its critical downstream targets may

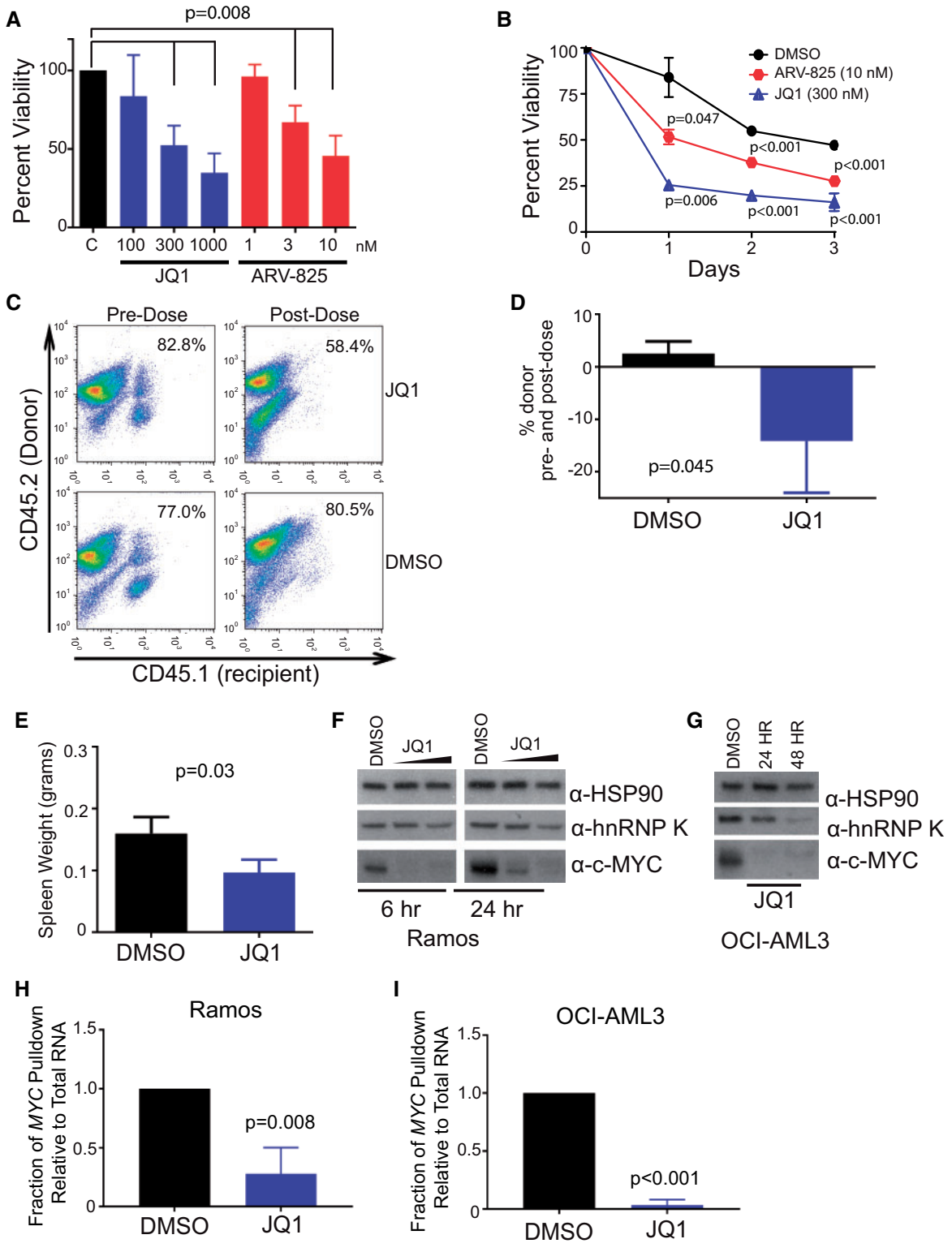

Figure 7. Utility of bromodomain inhibitors in hnRNP K-dependent lymphomas. **A)** Bar graph depicting cell viability in splenocytes isolated from tumor-burdened *Eμ-Hnrnpk* mice (n = 5) following treatment with increasing doses of JQ1 (100, 300, and 1000 nM) and ARV-825 (1, 3, and 10 nM). Data are represented as the mean ± SD. Samples were compared with their corresponding DMSO controls to obtain *P* values, which were calculated using a two-sided Mann-Whitney test. **B)** Viability of splenocytes isolated from tumor-burdened *Eμ-Hnrnpk* mice (n = 3) following treatment with JQ1 (300 nM) and ARV-825 (3 nM) for 24, 48, and 72 hours. Data are represented as the mean ± SD. Samples were compared with their corresponding DMSO controls to obtain *P* values, which were calculated using a two-sided Student *t* test. **C and D)** Flow cytometry analysis of $CD45.1^+$ (recipient) and $CD45.2^+$ (donor) hematopoietic cells in the peripheral blood before (**left panels**) and after (**right panels**) following JQ1 treatment (**top panels**) and DMSO (**bottom panels**). Data are represented as the mean ± SD. *P* values were calculated using a two-sided Student *t* test. **E)** Bar graph depicting the splenic weight of transplanted NSG mice following JQ1 or vehicle treatment. Data are represented as the mean ± SD. *P* values were calculated using a two-sided Student *t* test. **F and G)** Immuno blot analysis of hnRNP K and c-Myc levels on JQ1 treatment in Ramos and OCI-AML3 cells, respectively. **H and I)** Bar graphs showing the amount of *MYC* immunoprecipitated by hnRNP K on DMSO or JQ1 treatment in Ramos and OCI-AML3 cells, respectively. Data are represented as the mean ± SD, after normalization to internal control RPLP0, as determined from four samples. *P* values were calculated using a two-sided Student *t* test. DMSO = dimethyl sulfoxide; hnRNP K = heterogeneous nuclear ribonucleoprotein K.

ARTICLE

represent a viable therapeutic strategy. Because no established hnRNP K-specific therapies currently exist and given hnRNP K's relationship with c-Myc, and the notion that c-Myc can be indirectly targeted with BET-bromodomain inhibitors (eg, JQ1 and ARV-825), we evaluated the efficacy of BRD4 inhibition. Bromodomain inhibition was efficacious in our model system, resulting in a decrease in c-Myc levels and reduced disease burden. Surprisingly, we also observed that JQ1 affects hnRNP K protein levels via a mechanism that remains to be determined. These results suggest that BET-bromodomain inhibitors could be an effective therapeutic modality in the treatment of malignancies characterized by hnRNP K overexpression, particularly when c-Myc levels are elevated secondarilyy to increased hnRNP K.

Given the dual functionality of hnRNP K and the fact that its bevy of functions have not been fully elucidated, there are some limitations to our study. This point is highlighted by the fact that hnRNP K has the capacity to regulate gene expression and signaling pathways beyond MYC. Thus, much work remains to fully understand how hnRNP K affects disease progression. Secondly, both overexpression and reduced expression of hnRNP K have been implicated in various malignancies, yet it remains enigmatic whether cell context or differentiation states affect the oncogenic or tumor-suppressive functions of hnRNP K in a given setting. Finally, given the retrospective nature of our clinical observations, future studies will be useful to assess the levels and role of hnRNP K in patients at different stages of disease and/or treatment.

In summary, our findings provide strong evidence that wild-type hnRNP K behaves as an oncogene when overexpressed. From a clinical perspective, hnRNP K overexpression may represent a novel mechanism for stimulating c-Myc expression in the absence of *MYC* alterations. This could have far-reaching implications for lymphoma patients, particularly those who do not harbor MYC amplifications or translocations and may benefit from hnRNP K screening for the purpose of risk stratification or potential inclusion in clinical trials using BET-bromodomain inhibitors. Finally, the challenge of improving outcomes for patients with DLBCL and other hnRNP K-overexpressing malignancies emphasizes the need to better understand the biology of this dual oncogene/tumor suppressor.

Funding

This work was supported by funding from a National Cancer Institute Cancer Center Support grant (CA016672) to the Veterinary and Pathology Core Facilities, Flow Cytometry and Cellular Imaging Facility, Proteomics Core, Sequencing and Microarray Facility, and Genetically Engineered Mouse Facility at MD Anderson Cancer Center. This investigation has been aided by a grant from the Jane Coffin Childs Memorial Fund for Medical Research (PM), a National Cancer Institute/National Institutes of Health Award (R01CA207204), Leukemia and Lymphoma Society (6577–19), and MDACC start-up funds (SMP). M-HW and HS were supported by the CPRIT Research Training program (CRP170067 and RP17067/RP140106, respectively). KHY was supported by the National Cancer Institute/National Institutes of Health (R01CA138688 and 1RC1CA146299). JM-L was supported by the Cancer Research Innovation Spain. MJLA is a recipient of the Dr John J. Kopchick Fellowship.

Notes

Affiliations of authors: Department of Leukemia (MG, PM, MJLA, XZ, M-HW, HM, RJ, HS, SMP), MD Anderson Cancer Center UTHealth Graduate School of Biomedical Sciences (MJLA), Department of Genomic Medicine (TML), Department of Epigenetics and Molecular Carcinogenesis (VS, MCB), Department of Molecular Oncology (SA, DS), Department of Veterinary Medicine and Surgery (LRP), Department of Hematopathology (LY, ZYX-M, CB-R, KHY), Department of Lymphoma and Myeloma, The University of Texas, MD Anderson Cancer Center, Houston, TX (HJL); Department of Hematology, Hospital Universitario Madrid, Spain (IR, JM-L); H12O-CNIO Haematological Malignancies Clinical Research Unit, Clinical Research Programme, CNIO, Madrid, Spain (MG).

The funders had no role in the design of the study; the collection, analysis, or interpretation of the data; the writing of the manuscript; or the decision to submit the manuscript for publication. The authors have no conflicts of interest to disclose.

Author contributions: MG and PM performed experiments, analyzed and interpreted data, and wrote the manuscript. MJLA performed experiments, analyzed and interpreted data, and critically revised the manuscript. XZ performed experiments, analyzed and interpreted data, supported the experimental procedures, and critically revised the manuscript. TML performed experiments, analyzed and interpreted data, and wrote the manuscript. VS analyzed and interpreted data. SA, M-HW, IR, HS, LY, and ZYX-M performed experiments. HM maintained mouse colonies and performed experiments. RJ generated cell lines and performed experiments. HJL performed experiments, analyzed and interpreted data, and revised the manuscript. DS supported research design. LRP performed and analyzed pathology studies. MCB analyzed data and supported research design. JM-L, CB-R, and KHY provided patients samples, performed experiments, and analyzed and interpreted data. SMP designed and supervised research and experiments, performed experiments, analyzed and interpreted data, and wrote the manuscript. All authors reviewed and accepted the manuscript. MG and PM contributed equally to this work.

We thank J. Bradner and Arvinas for the bromodomain inhibitors, JQ1 and ARV-825, respectively.

References

1. Barboro P, Ferrari N, Balbi C. Emerging roles of heterogeneous nuclear ribonucleoprotein K (hnRNP K) in cancer progression. *Cancer Lett*. 2014;352(2):152–159.
2. Bomsztyk K, Denisenko O, Ostrowski J. hnRNP K: one protein multiple processes. *Bioessays*. 2004;26(6):629–638.
3. Chen X, Gu P, Xie R, et al. Heterogeneous nuclear ribonucleoprotein K is associated with poor prognosis and regulates proliferation and apoptosis in bladder cancer. *J Cell Mol Med*. 2017;21(7):1266–1279.
4. Enge M, Bao W, Hedström E, Jackson SP, Moumen A, Selivanova G. MDM2-dependent downregulation of p21 and hnRNP K provides a switch between apoptosis and growth arrest induced by pharmacologically activated p53. *Cancer Cell*. 2009;15(3):171–183.
5. Gallardo M, Hornbaker MJ, Zhang X, Hu P, Bueso-Ramos C, Post SM. Aberrant hnRNP K expression: all roads lead to cancer. *Cell Cycle*. 2016;15(12):1552–1557.
6. Moumen A, Masterson P, O'Connor MJ, Jackson SP. hnRNP K: an HDM2 target and transcriptional coactivator of p53 in response to DNA damage. *Cell*. 2005;123(6):1065–1078.
7. Carpenter B, McKay M, Dundas SR, Lawrie LC, Telfer C, Murray GI. Heterogeneous nuclear ribonucleoprotein K is over expressed, aberrantly localised and is associated with poor prognosis in colorectal cancer. *Br J Cancer*. 2006;95(7):921–927.
8. Gao R, Yu Y, Inoue A, Widodo N, Kaul SC, Wadhwa R. Heterogeneous nuclear ribonucleoprotein K (hnRNP-K) promotes tumor metastasis by induction of

ARTICLE

genes involved in extracellular matrix, cell movement, and angiogenesis. *J Biol Chem*. 2013;288(21):15046–15056.
9. Wang F, Zhang P, Shi C, Yang Y, Qin H. Immunohistochemical detection of HSP27 and hnRNP K as prognostic and predictive biomarkers for colorectal cancer. *Med Oncol*. 2012;29(3):1780–1788.
10. Lynch M, Chen L, Ravitz MJ, et al. hnRNP K binds a core polypyrimidine element in the eukaryotic translation initiation factor 4E (eIF4E) promoter, and its regulation of eIF4E contributes to neoplastic transformation. *Mol Cell Biol*. 2005;25(15):6436–6453.
11. Adolph D, Flach N, Mueller K, Ostareck DH, Ostareck-Lederer A. Deciphering the cross talk between hnRNP K and c-Src: the c-Src activation domain in hnRNP K is distinct from a second interaction site. *Mol Cell Biol*. 2007;27(5):1758–1770.
12. Zhang X, Pageon L, Post SM. Impact of the Mdm2SNP309-G allele on a murine model of colorectal cancer. *Oncogene*. 2014;34(33):4412–4420.
13. Shaw AC, Swat W, Ferrini R, Davidson L, Alt FW. Activated Ras signals developmental progression of recombinase-activating gene (RAG)-deficient pro-B lymphocytes. *J Exp Med*. 1999;189(1):123–129.
14. G Hendrickson D, Kelley DR, Tenen D, Bernstein B. Rinn JL. Widespread RNA binding by chromatin-associated proteins. *Genome Biol*. 2016;17(1):28.
15. Eason AB, Sin S-H, Lin C, et al. Differential IgM expression distinguishes two types of pediatric Burkitt lymphoma in mouse and human. *Oncotarget*. 2016;7(39):63504–63513.
16. Mori S, Rempel RE, Chang JT, et al. Utilization of pathway signatures to reveal distinct types of B lymphoma in the Emicro-myc model and human diffuse large B-cell lymphoma. *Cancer Res*. 2008;68(20):8525–8534.
17. Rempel RE, Jiang X, Fullerton P, et al. Utilization of the Eμ-Myc mouse to model heterogeneity of therapeutic response. *Mol Cancer Ther*. 2014;13(12):3219–3229.
18. Wen R, Chen Y, Bai L, et al. Essential role of phospholipase C gamma 2 in early B-cell development and Myc-mediated lymphomagenesis. *Mol Cell Biol*. 2006;26(24):9364–9376.
19. Lv X, Feng L, Ge X, Lu K, Wang X. Interleukin-9 promotes cell survival and drug resistance in diffuse large B-cell lymphoma. *J Exp Clin Cancer Res*. 2016;35(1):106.
20. Michelotti EF, Michelotti GA, Aronsohn AI, Levens D. Heterogeneous nuclear ribonucleoprotein K is a transcription factor. *Mol Cell Biol*. 1996;16(5):2350–2360.
21. Mikula M, Bomsztyk K, Goryca K, Chojnowski K, Ostrowski J. Heterogeneous nuclear ribonucleoprotein (HnRNP) K genome-wide binding survey reveals its role in regulating 3′-end RNA processing and transcription termination at the early growth response 1 (EGR1) gene through XRN2 exonuclease. *J Biol Chem*. 2013;288(34):24788–24798.
22. Sadelain M, Papapetrou EP, Bushman FD. Safe harbours for the integration of new DNA in the human genome. *Nat Rev Cancer*. 2011;12(1):51.
23. Forbes SA, Beare D, Boutselakis H, et al. COSMIC: somatic cancer genetics at high-resolution. *Nucleic Acids Res*. 2017;45(D1):D777–D783.
24. Kramer MHH, Hermans J, Wijburg E, et al. Clinical relevance of BCL2, BCL6, and MYC rearrangements in diffuse large B-cell lymphoma. *Blood*. 1998;92(9):3152–3162.
25. Ott G, Rosenwald A, Campo E. Understanding MYC-driven aggressive B-cell lymphomas: pathogenesis and classification. *Blood*. 2013;122(24):3884–3891.
26. Xu-Monette ZY, Dabaja BS, Wang X, et al. Clinical features, tumor biology, and prognosis associated with MYC rearrangement and Myc overexpression in diffuse large B-cell lymphoma patients treated with rituximab-CHOP. *Mod Pathol*. 2015;28(12):1555–1573.
27. Evans JR, Mitchell SA, Spriggs KA, et al. Members of the poly (rC) binding protein family stimulate the activity of the c-myc internal ribosome entry segment in vitro and in vivo. *Oncogene*. 2003;22(39):8012.
28. Filippakopoulos P, Qi J, Picaud S, et al. Selective inhibition of BET bromodomains. *Nature*. 2010;468(7327):1067–1073.
29. Lu J, Qian Y, Altieri M, et al. Hijacking the E3 ubiquitin ligase cereblon to efficiently target BRD4. *Chem Biol*. 2015;22(6):755–763.
30. Mertz JA, Conery AR, Bryant BM, et al. Targeting MYC dependence in cancer by inhibiting BET bromodomains. *Proc Natl Acad Sci U S A*. 2011;108(40):16669–16674.
31. Delmore JE, Issa GC, Lemieux ME, et al. BET bromodomain inhibition as a therapeutic strategy to target c-myc. *Cell*. 2011;146(6):904–917.
32. Gallardo M, Lee HJ, Zhang X, et al. hnRNP K is a haploinsufficient tumor suppressor that regulates proliferation and differentiation programs in hematologic malignancies. *Cancer Cell*. 2015;28(4):486–499.
33. Krönke J, Bullinger L, Teleanu V, et al. Clonal evolution in relapsed NPM1-mutated acute myeloid leukemia. *Blood*. 2013;122(1):100–108.
34. Au PYB, You J, Caluseriu O, et al. GeneMatcher aids in the identification of a new malformation syndrome with intellectual disability, unique facial dysmorphisms, and skeletal and connective tissue abnormalities caused by de novo variants in HNRNPK. *Hum Mutat*. 2015;36(10):1009–1014.
35. Ley TJ, Miller C, Ding L, et al. Genomic and epigenomic landscapes of adult de novo acute myeloid leukemia. *N Engl J Med*. 2013;368(22):2059–2074.
36. Dentici ML, Barresi S, Niceta M, et al. Clinical spectrum of Kabuki-like syndrome caused by HNRNPK haploinsufficiency. *Clin Genet*. 2018;93(2):401–407.
37. Lange L, Pagnamenta AT, Lise S, et al. A de novo frameshift in HNRNPK causing a Kabuki-like syndrome with nodular heterotopia. *Clin Genet*. 2016;90(3):258–262.
38. Naarmann-de Vries IS, Sackmann Y, Klein F, et al. Characterization of acute myeloid leukemia with del(9q) – impact of the genes in the minimally deleted region. *Leuk Res*. 2019;76:15–23.
39. Notari M, Neviani P, Santhanam R, et al. A MAPK/HNRPK pathway controls BCR/ABL oncogenic potential by regulating MYC mRNA translation. *Blood*. 2006;107(6):2507–2516.
40. Wen F, Shen A, Shanas R, et al. Higher expression of the heterogeneous nuclear ribonucleoprotein K in melanoma. *Ann Surg Oncol*. 2010;17(10):2619–2627.
41. Wu C-S, Chang K-P, Chen L-C, et al. Heterogeneous ribonucleoprotein K and thymidine phosphorylase are independent prognostic and therapeutic markers for oral squamous cell carcinoma. *Oral Oncol*. 2012;48(6):516–522.
42. Ritchie SA, Pasha MK, Batten DJP, et al. Identification of the SRC pyrimidine-binding protein (SPy) as hnRNP K: implications in the regulation of SRC1A transcription. *Nucleic Acids Res*. 2003;31(5):1502–1513.